# A Future Proof Reconfigurable Wireless and Fixed Converged Optical Fronthaul Network Using Silicon Photonic Switching Strategies

Junfei Xia, *Student Member, IEEE*, Tongyun Li, *Member IEEE*, Qixiang Cheng, *Member IEEE*, Madeleine Glick, *Senior Member, IEEE*, Michael Crisp, *Member, IEEE*, Keren Bergman, *Fellow, IEEE*, and Richard Penty, *Senior Member, IEEE*

***Abstract*—Broadband access services in the era of 5G and beyond are driving the evolution of optical access networks from a fiber-to-the-home/ fiber-to-the-building infrastructure to a more common access platform, compatible with both wired and wireless broadband services. Accordingly, a flexible optical access network plays a pivotal role in catering to various service requirements. This work proposes a reconfigurable converged optical fronthaul network for wireless and wired services using a 4×4 microring resonator (MRR) based silicon photonic (SiP) switch fabric. Reconfigurable service selection is demonstrated for wavelength selective, multicast and space switching scenarios. The reconfiguration of digital data and digital radio-over-fiber (DRoF) services for cloud radio access networks (C-RAN) is demonstrated.**

***Index Terms*—Passive optical networks, optical fiber networks, Optical switches, photonic integrated circuits, radio access networks, silicon photonics.**

## I. Introduction

The explosive growth in mobile connectivity and high-performance computing continue to drive global internet traffic demands. A report from Cisco predicts that over 70 percent of the global population will own mobile handsets, and that fifth-generation (5G) mobile technology will be deployed on 10 percent of mobile devices by 2023 [1]. To support this, the transport network must provide higher bandwidth and lower latency to enable extensive scalability and flexibility in selecting different services. This leads to a requirement for reconfigurable networks able to support fixed data services alongside wireless access networks.

Looking towards 6G, mobile service providers are gradually adopting new services with millimetre-wave / Terahertz frequencies, massive multiple-input and multiple-output and carrier aggregation technologies to further enhance mobile throughput. Future 6G systems are expected to support a 200Gb/s peak rate, a density of 10M connections/ km$^2$, 500EB/ month traffic, a 300GHz frequency spectrum, and a latency level down to 100μs [2]. In addition to unforeseen applications, 6G will support applications such as autonomous driving systems, intelligent robotics and last-mile delivery, the optical access network with lower latency, higher flexibility and manageability[3].

Centralized Cloud Radio Access Network (C-RAN) has been proposed as a promising architecture to facilitate the management of complex mobile networks, significantly increasing efficiency and reducing energy consumption and costs [4]. In particular, C-RAN aggregates the mobile/radio-access network equipment at a Central Office (CO) and Remote Radio Units (RRU) at distributed antenna sites. A fiber optic fronthaul, with advantages of high bandwidth and low latency, provides the connections between the CO and each RRU. However, the fronthaul network has been largely static with fixed Base Band Units (BBU) to RRU mapping. BBU in C-RAN is moving into edge data centers (EDC) [5], requiring a large-scale integrated switching platform, which allows both conventional data and fronthaul services to be consolidated.

Digital radio over fiber (DRoF) is preferred for front hauling current mobile communications standards due to its high signal fidelity enabling greater RF spectral efficiency. This comes at the cost of poor spectral efficiency in the optical domain, where 1.2Gbps is required for a single 20MHz LTE channel. Analog radio over fiber (ARoF) is seeing a resurgence of interest for wideband applications due to its greater spectral efficiency within the fronthaul. Therefore, it is critical that a flexible front haul network support both analog and digital RF signal transmission.

While C-RAN is efficient for sharing hardware resources in the mobile network, a standalone fronthaul link for each RRU is not feasible for an extensive network. C-RAN fronthaul can be implemented over traditional passive optical networks (PON) to reduce power consumption in a 6G-based solution [2]. By using multi-casting, wavelength or spatial switching, a C-RAN fronthaul network can be created, enabling a software-defined network and resource sharing and radio processing. In C-RAN, optical fronthaul links using Digital Radio over Fiber (DRoF) solutions (i.e. carrying digitized Radio Frequency (RF) services) are converging with traditional data infrastructures such as Ethernet by mapping the Common Public Radio Interface (CPRI) or evolved CPRI (eCPRI) protocols into Ethernet frames [6], [7]. However, high capacity and stringent latency requirements are major obstacles to the practical

Manuscript received June X, 2021; revised XXXX; accepted March 24, 2020. Date of publication April 2, 2020; date of current version October 1, 2020. This work was supported by XXXX under XXXX (*Corresponding author: Junfei Xia*)

Junfei Xia, Tongyun Li, Qixiang Cheng, Michael Crisp and Richard Penty are with the Electrical Engineering Division, Department of Engineering, University of Cambridge, Cambridge University, Cambridge CB3 0FA, U.K (e-mail: jx248@cam.ac.uk; tl299@cam.ac.uk; mjc87@cam.ac.uk; qc223@cam.ac.uk; rvp11@cam.ac.uk)

Keren Bergman is with the Department of Electrical Engineering, Columbia University, New York, NY 10027 USA (email: bergman@ee.columbia.edu)

Color versions of one or more of the figures in this article are available online at http://ieeexplore.ieee.org.

Digital Object Identifier XXXXXXXX

deployment of converged fronthaul and fixed wired access over Ethernet due to the excessive overheads and timing issues caused by packet switching. This is partially addressed with various functional splits defined in eCPRI to offer reduced data rate and increased latency options to reduce the fronthaul requirements. Yet, this increases the RRU complexity, and vendor-specific information is required. Advanced functionalities such as coordinated multipoint communication are heavily restricted or not possible in such implementations.

Convergence could be enabled by a reconfigurable silicon photonic (SiP) optically switched network in the fronthaul link between virtualized BBUs and RRUs [8], [9]. Additionally, due to its scalable integration, low latency and the flexibility of wavelength and space switching, SiP switching technology could provide the co-management of fixed service Optical Line Terminals (OLTs) and wireless service BBUs by connecting both through a common large-scale switching infrastructure using software controls [10].

Recent research demonstrates the use of SiP technologies in converged optical networks. Our previous work has described the feasibility of using a SiP switching platform for DRoF in optical fronthaul links [11]. C. Browning *et al.* investigated the ability of a differential drive SiP Mach-Zehnder Modulator (MZM) and Micro-ring resonator (MRR) based SiP switch to support efficient ARoF service [12], [13], [14]. V. Sorianello *et al.* reported 10Gb/s CPRI transmission on 12 Wavelength Division Multiplexing (WDM) channels based on a SiP Reconfigurable Optical Add Drop Multiplexer (ROADM) realized by tunable MRRs [15]. P. Ionvanna *et al.* depicted an MRR-based ROADM and a flexible WDM hub implemented in a DRoF-based C-RAN [16].

The feasibility of the co-existence of DRoF services and data services was previously proposed in Ref [17] in a converged optical fronthaul network, using wavelength switching functionality. However, the switch-and-select MRR enables switching in wavelength and space. In this work, we for the first time propose and demonstrate an integrated MRR-based silicon photonic switching architecture for DRoF fronthaul, capable of multiplexing, multi-casting, and switching multiple wired and wireless services with reconfigurability. As the MRR-based switch is designed as a flexible space-and-wavelength switch, it simultaneously facilitates space, wavelength selection, and multicast operation. This could have a profound impact on fronthaul solutions in which flexible and reconfigurable network topology and interfaces with existing transport networks could be created at the mobile edge. Together with data compression, the digital RF (1/3 rate of CPRI) and data services are transmitted using a single SiP switch chip in a spectrally-efficient manner under all three switching scenarios. We also prove that the fronthaul system is scalable through the dynamic range performance, which potentially supports >100 port counts or 2.5Tbps compressed fronthaul throughput (25Gbps each channel) using a single integrated chip.

## II. The Design of Reconfigurable Wireless and Fixed Converged Optical Access Network

A future C-RAN concept was recently proposed by leveraging next-generation WDM-PON infrastructure, which supports C-RAN on the current existed PON via wavelength (de-)multiplexing[18]. However, the envisaged C-RAN/ PON cannot simultaneously achieve space and wavelength switching functionalities. SiP platform is then the key enabler to have WDM flexibility and space switch capability [19], [20], which can provide either route or wavelength selection in the converged network.

This novel design of a converged optical access network satisfies the requirements of increased network flexibility in the optical domain, as well as proposed convergence among mobiles and cloud access. The schematic of our reconfigurable wireless and fixed converged optical access network is shown in Fig. 1, where different wavelengths can be dynamically switched to different RRUs. In particular, the optical switching fabric is connected to centralized BBUs and Optical Line Terminals (located in the CO), providing wireless services by the remote antennas and fixed data communication by remote Optical Networking Units (ONU).

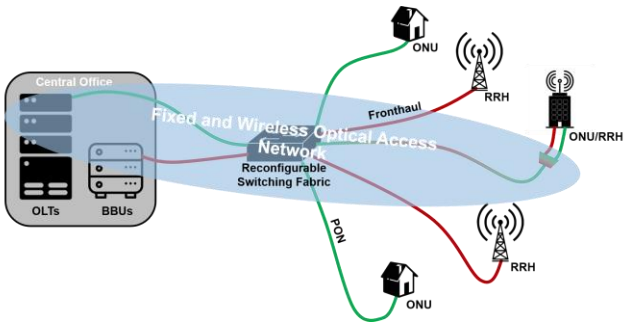


Fig. 1. The proposed reconfigurable converged optical access network concept for fixed and wireless services (red curve and green curve represent the wireless and fixed services, respectively).

## III. Multi-functional Integrated Switching Scenarios

### A. Switch fabric and device characterization

The switch-and-select architecture is applied to the design of the SiP chip, including two add/drop linear switching arrays connected via a passive shuffle network. As shown in Fig 2(a), each array is constructed by *N* 1x*N* / *N*x1 switching units with assembled MRR add-drop filters performing as (de-)multiplexers. The resonances of the MRRs can be tuned thermally by varying drive voltages to select the required add/drop wavelengths. By tuning pairs of MRRs in the two switching arrays, the switch can provide strictly non-blocking connectivity and form a specific spatial and wavelength selected input/output path.

The 4x4 SiP MRR-based switch-and-select layout is depicted in Fig 2(b). This device is similar to the previous work reported in [21]. To eliminate reflections, optical terminations are set at each through port. A shuffle network is designed with multi-mode waveguide crossings for low-loss and low-crosstalk. The thermo-optic MRRs are placed at a pitch of 100μm to minimize

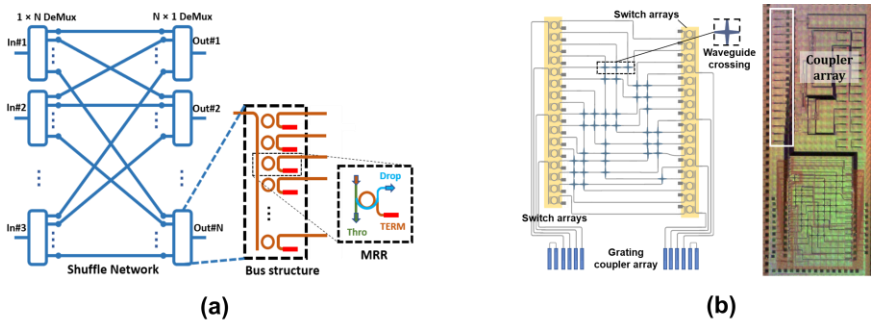


Fig 2(a) NxN switch-and-select topology with MRR-based elements. (b) Schematic of a silicon 4x4 MRR-based switch (reprinted from [12]).

thermal crosstalk. The measured resonance shift shows a thermal efficiency of 1nm/mW [22]. Approximately 24GHz bandwidth for 3dB passbands is also observed [18].

The device was taped out using standard Process Design Kit (PDK) elements through the AIM Photonics MPW run [23]. The switch fabric has a compact footprint of 1.6 x 2.5mm$^2$ with 34 electrical bonding pads. The fabricated device was die-bonded onto a chip carrier and mechanically clamped on a 3M QFN test socket. A custom printed circuit board for electrical fan-out was designed, and a standard grating coupler array is configured with a pitch of 127um, where the fiber array with a polished angle of 8 degrees is bonded onto the platform to couple TE-mode optical signal into/from the chip.

The experimental work used tunable lasers operating at 1538.65nm and 1540.16nm. It is notable that the wavelengths support the downlink whereas the uplink takes place at O-band (1310nm). Another specifically designed switch at O-band is required, but it can be integrated with the current switch within a single footprint. In this paper, we noted the performance of the C-band silicon because the specification of the O-band platform shows very similar optical properties to C-band. The measured on-chip loss is in the range of 2.3 to 4.8dB. The passive loss of each path comes from different loss sources, including micro-ring drop and through loss, waveguide bending, crossing and propagation loss. A looped pair of edge couplings measured the coupling loss at 6dB/facet. The switch crosstalk ratio is in the range of -57dB to -48.5dB [20].

### *B. Flexible switch modalities*

The experimental work uses three switching scenarios to evaluate the downlink performance of the proposed fronthaul and data service. The uplink operation could also be achieved using different wavelengths and spatial routes through the switch, but the performance would be similar. The schematic of a switching route including downlink and uplink is depicted in Fig 3. Two optical circulators are applied in the system at both BBU and RRU sides for downlink and uplink transmission for directional transmission isolation. Optical amplifiers are employed at the receiver of BBU/RRU for loss compensation. As the switch is not directional in the uplink, the ONU/RRU side of the switch can remain the same by effectively reversing the inputs and outputs to simplify cabling, where the switch can route the uplink signals back to the BBU pools. The following switch scenarios chosen as downlinks demonstrate the full wavelength and spatial routing capabilities of the switch.

#### *1) Scenario 1: Wavelength Selective Switching*

The consolidation of C-RAN and PON architecture can be achieved by Reconfigurable Arrayed Waveguide Grating (R-AWG) or mini-ROADMs. The fundamental topology is a point-to-multipoint network that can offer dynamic connectivity at a remote node stage [8]. 5G has the further demands on higher bandwidth, lower latency and greater flexibility when more wired or wireless services are jointly deployed within this network [24]. The switch fabric in this scenario is compatible with WDM, and wavelength selective switching can route different wavelengths on the same input port to different spatial outputs, as shown in Fig 3(b). BBU and OLT signals are modulated onto two different wavelengths while a simple, wavelength insensitive combiner results in a 3-dB loss. Either wavelength can be selected at the switch and sent to the appropriate receivers of either ONUs or RRUs.

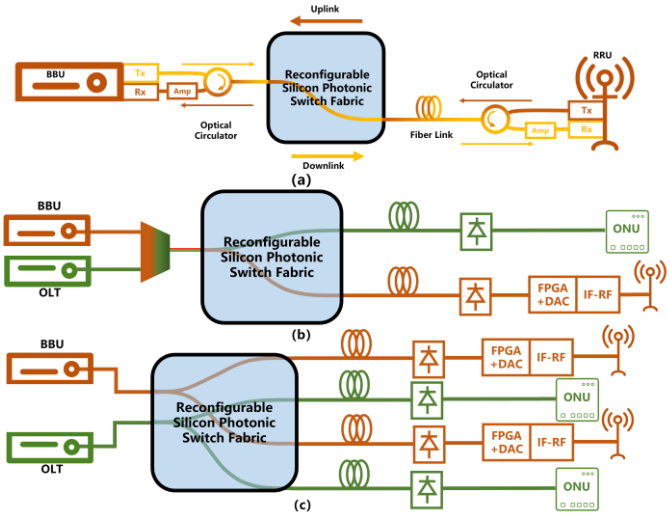


Fig 3 (a) Schematic of switching route BBU to RRUs with downlink and uplink (b) Schematic of wavelength selective switching functionality with the co-existence of BBUs and OLTs. (c) Schematic of multicast switching functionality with 2 channels multicast from BBUs or OLTs.

#### *2) Scenario 2: Multicast Switching*

The MRR switch can be reconfigured to allow different services on the dedicated wavelengths to be split and broadcast to selected output ports, as depicted in Fig 3(c). By tuning each 1x4 MRR at the first stage, two or more rings in the MRR unit can be tuned as drop status accordingly by shifting the center wavelength of their passbands. Specifically, when the input wavelength comes into the 1x4 MRR bus with a number of configured as outputs, the power is partially dropped through the first MRR configured as an output, and the residual signal continues to be dropped at subsequent MRRs in the bus. This mechanism can be used in a single switching cell as a configurable 1xN splitter. It is noteworthy that the multicast switch can perform under the current PON standards with TDM

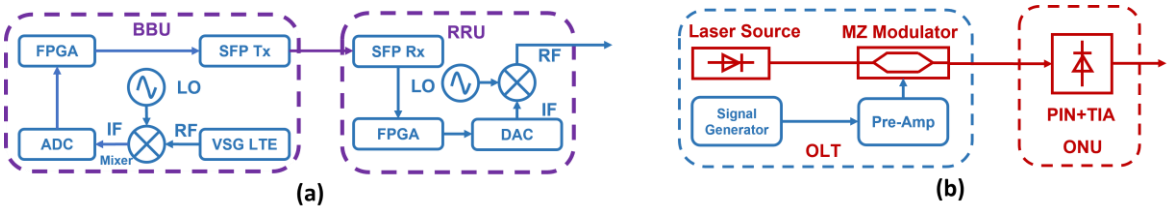


Fig 5. (a) Schematic block diagram of back-to-back system from BBU to RRU for DRoF service; (b)Schematic block diagram of back-to-back system from OLT to ONU for digital data service.

for the uplink, where inputs and outputs are reversely applied. 1x4 MRR at the BBU/OLT side is configured with two or more rings at drop status. The configuration can perform as a 4x1 combiner for TDM services. To achieve uniformity of the power splitting, precise voltage levels are required to drive the thermo-optic MRRs. Previous work [25] has demonstrated multi-casting functionality up to 3 output ports of a SiP MRR-based switch by a scalable software-defined control plane.

*3) Scenario 3: Space Switching*

In the CO, multiple BBU and OLTs pools are expected to be implemented in the switch network to further centralize the management, where the MRR switch fabric can offer space switching functionality. In particular, RF signals from BBUs could all be carried optically on a specific wavelength while OLTs adopt another optical carrier. 4x4 MRR switch has 16 optical routes; therefore, 32 tuning rings at the first and second stages are associated as 16 pairs to construct the optical route for a particular wavelength. In these two cases served for two different services, as shown in Fig 4(a) and 4(b), the switch can configure the space switching functionality as a "bar" or "cross" state to transmit the signal from different pool resources to the expected RRU or ONU ends.

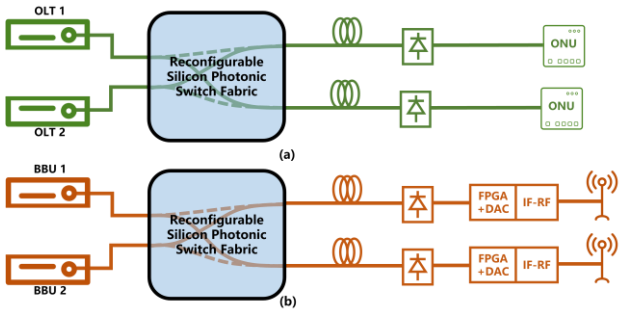


Fig 4. Schematic of space switching functionality for (a) two BBUs or (b) two OLTs with BBUs and OLTs each using a distinct wavelength.

## C. Wired and Wireless Services

*1) DRoF for converged fronthaul network:*

DRoF carries digitized Radio Frequency (RF) services over the optical fiber infrastructure [6]. Although the digitization degrades spectral efficiency and requires digital-to-analog conversion and packetization compared to analog radio-over-fiber, it provides higher tolerance to the noise and nonlinearities in the optical transmission network. To emulate the BBU, as shown in the back-to-back system in Fig. 5(a), an RF signal is initially generated using a vector signal generator (VSG) and then down-converted to an intermediate frequency (IF) using an RF mixer, followed by an analog-to-digital converter (ADC) that converts the signal to a digital format. Subsequently, the digitized RF is processed on a field-programmable gate array (FPGA) platform for data compression and packetization for transmission. An SFP+ module is used to transmit the FPGA processed data over an optical fiber. At the RRU, another FPGA is used for decompression and depacketization, and a digital-to-analog converter (DAC) is applied to recover the IF analog signal. An RF mixer and local oscillator up-converting back to the RF frequency for wireless transmission.

CPRI and eCPRI are interface options we can use, and ultimately we plan to build reconfigurable fronthaul units that can flexibly interface with multiple standards [6]. The drawback of CPRI is that the standard is still quite vendor-specific, which makes neutral hosting difficult. In addition, the overheads defined in CPRI also limit the compression ratio that is achieved without sacrificing the dynamic range performance. The compressive DRoF system offers another alternative approach to reduce the required data rate allowing flexible, efficient, and open fronthaul transmission. A multi-service DRoF system has been demonstrated with data compression, showing a 3-times reduction of data rate with no loss of the input power dynamic range [26]. The scheme has been applied to a converged distributed antenna system (DAS) for indoor wireless coverage and is now ready for commercial implementation [27]. However, a different approach will be required to realize the convergence of compressive DRoF and fixed wireless access.

This work emulates a DRoF service in the fronthaul link. A 20MHz 4G-LTE signal with 64 QAM and carrier frequency at 1.8GHz is transmitted through the network. Two identical RF mixers are placed for down-converting and up-converting to/from an IF of 37.5MHz at the RF frontend. A 14-bit 150MSPS ADC and DAC pair is deployed for converting the signals before digital signal processing in the FPGA. The digitized signal is compressed to 400Mbps per 20MHz bandwidth LTE service with data compression. Sixteen uncorrelated replica LTE streams are created and packetized into a serialized data channel with a line rate of 8 Gb/s with 8b/10b coding, which is equivalent to 320MHz spectral bandwidth or three 100MHz-bandwidth 5G services. 10G small form factor plus (SFP+) transceiver modules with distributed feedback laser (DFB) lasers are used for converting the signals onto optical carriers. The system can be easily scaled up upon the availability of 5G testing instruments.

*2) Data service in the passive optical networks:*

The PON is the dominant optical access network and will continue to be deployed in the context of 5G. Two main current PON standards are deployed: GPON based on ATM protocols and EPON focusing on native use of Ethernet [28]. Compared to the conventional PON point-to-multipoint topology, the switch used here can provide the functionality of optical distribution networks and dynamically configure the

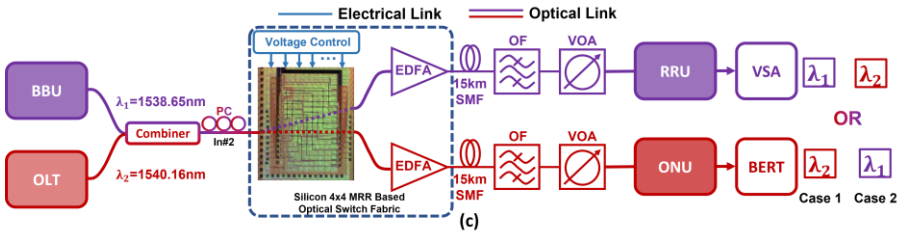


Fig 6. Experimental setup for scenario 1 with silicon MRR based switch (red lines and purple lines represent optical carriers at 1538.65nm and 1540.16nm, respectively).

transmission paths when an ONU requests connections to different OLT pools.

Fig 5(b) shows an emulated back-to-back link. To emulate an OLT in the PON, a Mach-Zehnder Modulator is used to modulate the 10GbE data service defined by the IEEE 802.3ae-2002 standard [29]. For the OLT, the digital electrical data is generated and then amplified with 20dB gain, by which the light from the tunable laser is subsequently modulated. At the ONU, a PIN-TIA converts the received optical signal to an electrical signal. The experiment carries 10Gb/s digital data as the fixed service in the PON transmission link.

## IV. Experimental Setup

In this work, the DRoF data is passed to SFP+ modules operating at a wavelength of 1538.65nm. 10Gb/s digital data service is modulated onto a tunable laser at 1540.16nm for all the scenarios discussed in Section III.B. Fig 6 shows the schematic of the experimental setup for the application in *Scenario 1*. Under all three scenarios, the light at the output of the switch is amplified by an Erbium-Doped Fiber Amplifier (EDFA) to compensate for the switch losses, which are in the range of 15dB - 20dB due to 12dB fiber coupling to/from the chip and 3dB on-chip loss. Both services are transmitted over a 15-km single-mode fiber (SMF) with an optical filter to remove ASE and an optical variable attenuator to adjust the received power before detection. At the receiver, a Vector Signal Analyzer (VSA) and Bit Error Rate Test (BERT) are used to analyze the error vector magnitude (EVM) of the RF service and the Bit Error Rate (BER) of the digital data service.

### A. System Characterization

As two optical carriers are applied to the switch fabric, the characterization of the switch fabric is measured under *Scenario 1* by using an optical spectrum analyzer to evaluate the switch extinction and crosstalk ratio. Fig 7(a) indicates the spectrum of output ports 1 and 2, whereas Fig 7(b) shows the amplified signal after the EDFA. Over 55dB switching extinction ratio can be achieved for both wavelengths at the output of the switch. Following the EDFA, the ratio is reduced to a level of ~40dB because of added ASE, indicating the feasibility of space switching applications. In Fig 7(a) and 7(b), below -35dB crosstalk ratio at the switch output port and below -34dB at EDFA output are observed, which is mainly attributed to wavelength multiplexing operation. These demonstrate that the switch can potentially be used under a wavelength selective switching scenario; however, lower cross talk is achieved for spatial switching.

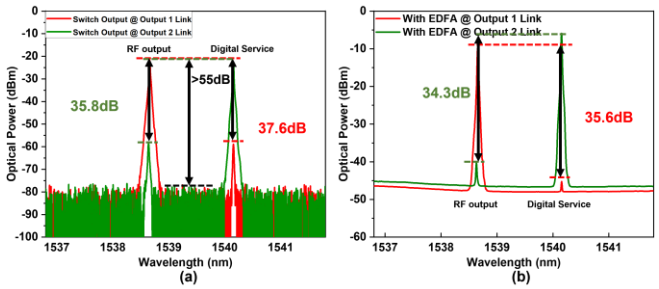


Fig 7. Optical carriers spectra for scenario 1 at (a) switch output ports (b) after EDFA amplification (red line at output port 1, green line at output port 2)

### B. Implementation of the Scenarios

*Scenario 1*: To evaluate the immunity of mutual influence between two types of services, measurements are comparably performed according to the cases for both services added or either of them dropped. In *Scenario 1*, each measurement is carried out with two routing cases – the first case is that DRoF is routed from input port 2 to output port 1 while switching the data service to output port 2; the second case is performed by exchanging two signals to the other output ports. For system settings, the DRoF signal and digital data service are multiplexed by an optical combiner with a 3.8dB loss, followed by a 0.2dB loss polarization controller. The combined signal is then fed to the switch fabric (input Port 2). The resonators are biased at ~2.9V and ~3.2V for the DRoF and digital data (due to the different wavelengths).

*Scenario 2*: The DRoF signal or digital data service are separately coupled to input port 2. Two rings of MRR bus associated with input port 2 and the rings associated with the input on output ports 1 and 2 are configured to on-state to maintain the identical power at each output. The multicast operation from input port 2 to output ports 1 and 2 is observed and compared to the operation without multicast.

*Scenario 3*: Space switching is implemented by applying two incoherent (DRoF or digital data service) optical signals of the same nominal wavelength to switch inputs (ports 1 and 2). By tunning the MRR elements, the switch is in "bar-state" (input port 1 to output port 1 while input port 2 to output port 2) and "cross-state" (input port 1 to output port 2 while input port 2 to output port 1) to deliver the services. The performance of the bar- and cross-states are compared with the two service types.

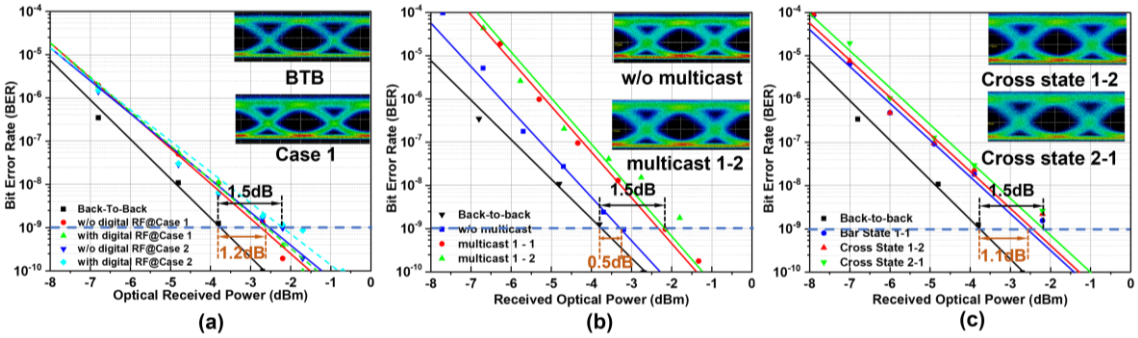


Fig 8. BER curves and eye diagrams for three scenarios. The insets show the received eye diagrams at a power level of -4dBm. (a) scenario 1 with/without digital RF channels under 2 switching cases. (b) scenario 2 with/without multicast operation. (c) scenario 3 with bar and cross switching states.

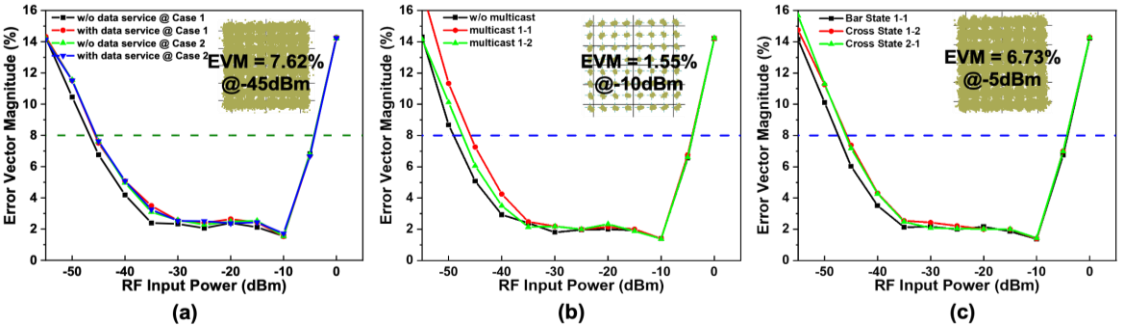


Fig 9. EVM vs RF input power with the received constellation digrams under three scenarios (a) scenario 1 with/without data service under 2 switching cases. (b) scenario 2 with/without multicast operation. (c) scenario 3 with bar and cross switching states.

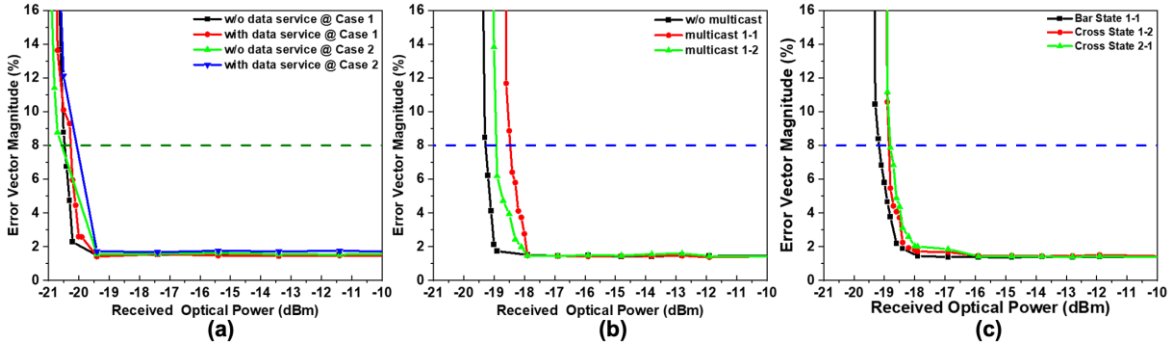


Fig 10. EVM vs received optical power under three scenarios. (a) scenario 1 with/without data service under 2 switching cases. (b) scenario 2 with/without multicast operation. (c) scenario 3 with bar and cross switching states.

## V. Results and Discussion

For 10Gb/s data service, a BER of $10^{-9}$ is considered the minimum acceptable threshold for data communication without Forward Error Correction (FEC), where the power penalty is evaluated. In RF links, by changing the input RF power in the electrical domain and the optical before the receiver, the DRoF service is investigated at 8% EVM (64-QAM requirement specified by 3GPP [30]). It is worth noting that the noise power of the receiver restricts the data transmission performance. Therefore, a higher received optical power is shown in the back-to-back data transmission to achieve the required BER in the data transmission link compared to the RF link. This power budget could be further increased to 26.2dB when an SFP+ Class C is applied. To follow up the development of PON towards 25/50G over the coming years. Advanced modulation formats can be applied in data transmission to achieve this high data rate due to a 24GHz switching passband. Recent progress shows that this SiP can achieve up to 53.6GHz with PAM-4 [37], and a 16x16 switching architecture can support 25Gb/s data transmission. The transmission of coherent signals is also required in PON upgrades, where quadrature amplitude modulation (QAM) is generally considered. The network involves polarization multiplexing technology, which requires a polarization-insensitive photonic switch. However, as the current designed polarization-insensitive switch can only achieve a low extinction ratio of -15dB [38], further improvements to the silicon photonic switch are required for the coherent communication in PON. Instead of polarization modulation, the other solution is implementing DWDM technologies for quadrature modulation, where both I and Q signals can be routed simultaneously and split with low crosstalk (<-30dB for adjacent channel isolation).

Fig 8 shows the BER curves under the three scenarios. For wavelength selective switching, the first and the second cases discussed in Section IV.B are depicted in Fig 8(a), with a power penalty of 1.2dB for the first case and 1.5dB for the second case. Compared to the condition without a multiplexed digital RF

service, the co-existence of RF and digital data service in both cases shows a 0.2dB penalty mainly attributed to wavelength crosstalk.

For the setup of multicast operation described in Section III.B.2, multicast channels from input port 1 to output port 1 (marked as multicast 1-1) and output port 2 (marked as multicast 1-2) are balanced to an equivalent output power level. The two channels show approximately identical performance with a power penalty of 1.5dB, as shown in Fig 8(b). Compared to multicast operation on two channels, a simple transmission shows a penalty of 0.5dB. It should be noted that when the number of multicast channels increases, optical signals are degraded by splitting the channels and thus bring about a power penalty of 1dB.

The best performance of space switching mentioned in Section III.B.3 is exhibited on the bar state, with a power penalty of 1.1dB, as indicated in Fig 8(c). The worst performance is a 1.5dB power penalty in cross-state from input port 2 to output port 1 (marked as Cross-State 2-1).

Fig 9 shows the RF input power dynamic range of each received RF channel. The range for downlink is related to the signal coverage of the RRUs. Two switching cases with or without data service are performed for wavelength selective switching and show over 40dB input power dynamic range as depicted in Fig 9(a). The minimum EVM achieved is 1.55%. For multicast switching indicated in Fig 9(b), the operation for RF signal multicast from input port 1 to output port 1 (marked as multicast 1-1) has a 42dB RF input power dynamic range. It is also notable that the dynamic range for the channel without multicast has 3dB more than that in multicast 1-1. The space switching is also exhibited in Fig 9(c), with a dynamic range of over 42dB. The figure insets show the received constellation diagrams with RF input power at -45/-10/-5dBm for scenarios (a), (b) and (c), respectively.

The evaluation of the RF input power dynamic range shows uniformity in performance under the three scenarios compared to the performance of the simple switching route. The multicast and space switching with the splitting loss and crosstalk sacrifice no more than 3dB dynamic range – effectively equalizing the power differentials and tolerating the variations in optical independent path crosstalk and losses.

Fig 10 depicts the optical received dynamic range for the three scenarios. The EVM under the three scenarios is also measured by varying the VOA as illustrated in Section IV, corresponding to received optical power. The rapid increase of EVM occurs when the optical power is attenuated to a critical power level, set by the sensitivity of the receiver. Specifically, Fig 10(a) indicates -19dBm is the worst case for wavelength selective switching where EVM increases above 8% suddenly. For multicast and space switching operations shown in Fig 10(b) and 10(c), the critical point of EVM >8% for their worst cases is -18dBm and -18.5dBm, respectively.

The maximum received power before detection is measured as -4dBm when the VOA is adjusted for minimum loss. This illustrates that at least a 14dB optical link budget is available in the wavelength selective switching scenario for future scaling up of the switch or longer propagation distance over fiber links. Improvements in fiber coupling [31] and the hybrid integration of III-V Semiconductor Optical Amplifier (SOA) on a silicon platform [32], [33] could alleviate the external amplification requirements for the proposed network.

While DRoF offers greater immunity to nonlinear distortion as well as noise and crosstalk due to the transmission of digital signals, the improvement in spectral efficiency given by ARoF is significant for future network scaling. This work demonstrates the feasibility of DRoF transmission for fronthaul transmission in the proposed centralized network. Some research has shown that the switch used in this paper can also be applied in an ARoF fronthaul system [13] and a hybrid ARoF and DRoF system for fronthaul application and has been demonstrated and achieved by coarse wavelength division multiplexing (C-WDM) [34] with wide dynamic range performance for both analog and digital RF services. The system is very similar to *Scenario 1* described in Section III.B.1, provisioning a reconfigurable and flat switching network for the co-existence of analog and digital RF transmission with wired services. A natural progression of this work is to design and implement a hybrid system which is a focus of our future work.

For future-proofing the centralized network to support more services, the proposed converged optical access network requires a high port count switching fabric to offer a scalable interaction between the central office pools and end-users. The tailored switch-and-select design maintains the number of drop micro-rings as a pair for any path while scaling up the switch through rings in the spatial (de-)multiplexers. The measured loss for the MRR drop and through states is 0.5dB and 0.1dB. This feature potentially yields silicon photonic switches with over 100 port counts for future scalable switching networks. With a 25Gbps data rate for each channel [37], 2.5Tbps data throughput can be achieved using a single integrated chip. Moreover, the development of gain-integration and flip-chip bond techniques to hybridize SOAs with silicon photonic switches can alleviate the EDFA amplification requirement and circumvent the insertion loss penalty [35], which can further scale up the port count of the switch by various switching cascading topology. This will be another focus of future study and is expected to significantly impact the converged network in 5G and beyond. Additionally, the proposed concept of the consolidation of 5G and PON, as a parallel split, is fitted in different layered network architectures with mapping of CU/DU/RU to PON in optical fronthaul architecture, as defined in ITU-T Series G Supplement 66 2020, which notes "the specific choice of the most suitable architecture would depend on specific deployment scenarios, the architecture can be further expanded to point-to-point, star, or tree topologies." [36]

## VI. Conclusion

The evolution of networks capable of providing high bandwidth and multiple types of services to our different devices will inevitably lead to the reconfigurable network for the converged fixed and wireless network. This work proposes a reconfigurable and converged network achieved by the SiP switch used. It can provide multiple functionalities for different data interaction scenarios, envisaging a compatible network on

the co-existence of fixed and wireless services between C-RAN and PON architectures.

Specifically, in a proof of principle experiment, for a 10Gb/s NRZ modulated digital data stream, power penalties in different scenarios do not exceed 1.5dB. In comparison, RF dynamic range is over 40dB for RF service, illustrating that wavelength (de-)multiplexing induced crosstalk, space switch-induced crosstalk, and splitting loss do not affect the transmission channels' performance. The 14dB optical link budget demonstrated could enable scaling up the switch port count to more than 100. Further expansion of port count can be realized by the heterogeneous integration of optical switches with SOAs. Overall, these results show that the co-existence of fixed and wireless services within a reconfigurable converged optical network achieved by SiP switch fabric can play diverse roles in C-RANs and PONs for the 5G and coming 6G era.

## ACKNOWLEDGEMENT

The author would acknowledge the ARPA-E ENLITENTED project (DE-AR00000843), PINE and EPSRC COALESCE project (Grant EP/P003990/1) for their funding support.

## REFERENCES

[1] Cisco, "Cisco Annual Internet Report (2018-2023)," 2020.
[2] T. R. Raddo *et al.*, "Transition technologies towards 6G networks," *Eurasip J. Wirel. Commun. Netw.*, Dec. 2021.
[3] I. T. Monroy *et al.*, "Testing Facilities for End-to-End Test of Vertical Applications Enabled by 5G Networks: Eindhoven 5G Brainport Testbed," in *International Conference on Transparent Optical Networks*, Sep. 2018.
[4] X. Wang *et al.*, "Virtualized Cloud Radio Access Network for 5G Transport," *IEEE Commun. Mag.* 2017,.
[5] Huawei, "5G-oriented Data Center Facility White Paper," 2016.
[6] N. J. Gomes *et al.*, "Fronthaul evolution: From CPRI to Ethernet," *Opt. Fiber Technol.*, vol. 26, pp. 50–58, Dec. 2015
[7] Z. Zakrzewski *et al.*, "D-RoF and A-RoF interfaces in an all-optical fronthaul of 5G mobile systems," *Appl. Sci.*, Feb. 2020.
[8] X. Guan *et al.*, "Silicon Photonics for 5G Passive Optical Networks," in *2019 IEEE 10th Annual Information Technology, Electronics and Mobile Communication Conference, IEMCON 2019*, Oct. 2019.
[9] B. Skubic *et al.*, "Rethinking optical transport to pave the way for 5G and the networked society," *J. Light. Technol.*, Mar. 2015.
[10] Q. Cheng *et al.*, "Recent advances in optical technologies for data centers: a review," *Optica*, 2018.
[11] J. Xia *et al.*, "Demonstration of Novel Silicon Optical Switching on Digital Radio over Fibre Link for Next-Generation Fronthaul," in *Conference on Lasers and Electro-Optics*, p. AW4M.1.
[12] C. Browning, "Wired and Wireless Convergence in Future Optical Access Networks - Invited," in *2019 IEEE Photonics Conference, IPC 2019 - Proceedings*, 2019.
[13] C. Browning *et al.*, "A Silicon Photonic Switching Platform for Flexible Converged Centralized-Radio Access Networking," *J. Light. Technol.*, 2020.
[14] C. Browning *et al.* "256/64-QAM Multicarrier Analog Radio-over-Fiber Modulation using a Linear Differential Drive Silicon Mach-Zehnder Modulator," Nov. 2018.
[15] V. Sorianello *et al.*, "Polarization insensitive silicon photonic ROADM with selectable communication direction for radio access networks," *Opt. Lett.*, 2016.
[16] P. Iovanna *et al.*, "Future proof optical network infrastructure for 5G transport," *J. Opt. Commun. Netw.*,Dec. 2016.
[17] J. Xia *et al.*, "Novel Scalable and Reconfigurable Optical Fronthaul Network for Converged Radio Frequency and Data Services Using Silicon Photonic Switching," in *OFC*, 2021, vol. F1D.3, pp. 6–8.
[18] J. I. Kani *et al.*, "Solutions for Future Mobile Fronthaul and Access-Network Convergence," *J. Light. Technol.*, Feb. 2017.
[19] M. Bahadori *et al.*, "Loss and crosstalk of scalable MZI-based switch topologies in silicon photonic platform," *2016 IEEE Photonics Conf. IPC 2016*.
[20] Q. Cheng *et al.*, "Scalable Microring-Based Silicon Clos Switch Fabric with Switch-and-Select Stages," *IEEE J. Sel. Top. Quantum Electron.*, Sep. 2019.
[21] Q. Cheng *et al.*, "Ultralow-crosstalk, strictly non-blocking microring-based optical switch," *Photonics Res.*, Feb. 2019.
[22] M. Bahadori *et al.*, "Thermal Rectification of Integrated Microheaters for Microring Resonators in Silicon Photonics Platform," *J. Light. Technol.*, Feb. 2018.
[23] "AIM Photonics."
[24] X. Liu *et al.*, "Emerging optical access network technologies for 5G wireless [invited]," *J. Opt. Commun. Netw.*,Dec. 2016.
[25] A. Gazman *et al.*, "Software-defined control-plane for wavelength selective unicast and multicast of optical data in a silicon photonic platform," *Opt. Express*, 2017.
[26] T. Li *et al.*, "Novel digital radio over fibre for 4G-LTE," in *2015 IEEE International Conference on Communication Workshop, ICCW 2015*,.
[27] W. Li et al., "Novel Digital Radio over Fiber (DRoF) System with Data Compression for Neutral-Host Fronthaul Applications," in *IEEE Access*, 2020.
[28] Malcolm Scott, "Protocols for Fibre to the Home," 2010.
[29] "802.3ae-2002 - IEEE Standard for Information technology.
[30] "Specification # 36.101."
[31] R. Marchetti *et al.*, "Coupling strategies for silicon photonics integrated chips [Invited]," *Photonics Res.*, 2019.
[32] M. Lamponi *et al.*, "Heterogeneously integrated InP/SOI laser using double tapered single-mode waveguides through adhesive die to wafer bonding," *IEEE Int. Conf. Gr. IV Photonics GFP*, 2010.
[33] T. Matsumoto *et al.*, "Hybrid-Integration of SOA on Silicon Photonics Platform Based on Flip-Chip Bonding," *J. Light. Technol.*, Jan. 2019,.
[34] T. Li *et al.* , "Novel Digital and Analogue Hybrid Radio over Fibre System for Distributed Antenna System (DAS) Fronthaul Applications," in *Conference on Lasers and Electro-Optics*, 2020, p. JTu2E.5.
[35] T. Matsumoto *et al.*, "In-line Optical Amplification for Silicon Photonics Platform by Flip-Chip Bonded InP-SOAs," *2018 Opt. Fiber Commun. Conf. Expo. OFC 2018 - Proc.*, 2018.
[36] "ITU-T Series G."
[37] D. Yuan, et al. "Experimental demonstration of PAM-4 transmission through microring silicon photonic Clos switch fabric." *2020 Opt. Fiber Commun. Conf. Expo. OFC 2020 - Proc.*, 2020.
[38] Yang, Huizhan, et al. "Broadband polarization-insensitive optical switch on silicon-on-insulator platform." *Optics Express* 26.11 (2018)